

iBlink: Smart Glasses for Facial Paralysis Patients

Sijie Xiong[†], Sujie Zhu[†], Yisheng Ji[†], Binyao Jiang[†], Xiaohua Tian[†],
Xuesheng Zheng[‡], Xinbing Wang[†]

[†]School of Electronic, Info. & Electrical Engineering, Shanghai Jiao Tong University, China

[‡]Xin Hua Hospital Affiliated to Shanghai Jiao Tong University School of Medicine, China

[†]{qq420778733, zhusujie, acetanil, emberspirit, xtian, xwang8}@sjtu.edu.cn,

[‡]pheiphei@126.com

ABSTRACT

Facial paralysis makes patients lose their facial movements, which can incur eye damage even blindness since patients are incapable of blinking. The paralysis usually occurs on just one side of the face, and clinical trials show that electrical stimulation could trigger blink. Based on such observations, we design and implement a pair of smart glasses *iBlink* to assist facial paralysis patients to blink. The basic idea is to monitor the normal side of the face with a camera and stimulate the paralysed side, so that the blink of the both eyes become symmetric. To the best of our knowledge, this is the first piece of wearable device for facial paralysis therapy.

Our contributions are: First, we propose an eye-blink detection mechanism based on deep convolutional neural network (CNN), which can detect asymmetric blinks of patients under various illumination conditions with an accuracy above 99%. Our eye-image library for training CNN models is published online for further related studies, which contains more than 30,000 eye images. Second, we design and implement an automatic stimulation circuits to generate electrical impulse for stimulating the patient's facial nerve branches, which can configure operational parameters in a self-adaptive manner for different patients. Third, we implement the entire *iBlink* system, which integrates the two functions above and a communication function module for tele-medicine applications. Moreover, we conduct clinical trials in a hospital, in order to obtain the design basis and verify effectiveness of our device.

CCS Concepts

•Computer systems organization → *Sensors and actuators*;

Keywords

Smart glasses; facial paralysis vfill

Permission to make digital or hard copies of all or part of this work for personal or classroom use is granted without fee provided that copies are not made or distributed for profit or commercial advantage and that copies bear this notice and the full citation on the first page. Copyrights for components of this work owned by others than ACM must be honored. Abstracting with credit is permitted. To copy otherwise, or republish, to post on servers or to redistribute to lists, requires prior specific permission and/or a fee. Request permissions from permissions@acm.org.

MobiSys'17, June 19-23, 2017, Niagara Falls, NY, USA

© 2017 ACM. ISBN 978-1-4503-4928-4/17/06...\$15.00

DOI: <http://dx.doi.org/10.1145/3081333.3081343>

1. INTRODUCTION

Facial paralysis is a disease making people losing facial movements, which is caused by nerve damage. People suffering from facial paralysis usually have muscles on one side of the face noticeably droop, which seriously impacts the person's quality of life. What is worse, facial paralysis can incur eye damage even blindness, because the eyelid on the affected side can not fully close, which makes the eye dry and infected by debris. The most common form of facial paralysis is known as Bell's palsy, which impacts 40,000 people in U.S. each year, where the typical symptom is the muscle dysfunction on one side of the face [1, 27].

Most Bell's palsy patients will completely recover in around 6 months with or without medical treatment; however, a few cases of facial paralysis patients could never completely return to normal. The current treatments for Bell's palsy include drugs and surgery, which is of side effect and controversial, respectively [1].

Efforts have been dedicated to find the cause of Bell's palsy; however, the exact cause is still unknown [1]. To the best of scientists' knowledge, the paralysis is due to the pressure incurred by infection in the tunnel containing main trunk of facial nerves, where the tunnel is inside of the people's head termed as the *Facial canal*. An interesting phenomenon corroborating the theory is: using electric current of 3 – 11mA to stimulate the facial nerve branches could make the eye closing for most of patients, which indicates that the facial muscle and nerve branches are still working.

In this paper, we propose to use wearable device to improve the facial paralysis patient's quality of life. In particular, we design and implement a pair of smart glasses *iBlink* to assist facial paralysis patients to blink. To the best of our knowledge, this is the first piece of wearable device for facial paralysis therapy. The basic idea of *iBlink* is to monitor the normal side of the face with a camera and stimulate the paralysed side, so that the blink of both sides of the face could become symmetric. As wearable devices such as Google glass are widely accepted, wearing *iBlink* could conceal the patient's defect and help them live like a normal people. Our contributions are as following:

First, we propose an eye-blink detection mechanism based on convolutional neural network (CNN), which can detect not only movements of eyes such as closing, opening and blink but also asymmetric blinks of facial paralysis patients under various lighting conditions even at night (§4.2). We collected more than 26,000 eye images under different illumination conditions and more than 7,750 images under infrared (IR) lights from 12 different people to train the CNN

models. The detection accuracies for daytime and nighttime are both above 99%. We publish the image library to support further related studies on facial paralysis [2].

Second, we design and implement an automatic stimulation circuits to generate electrical impulse for stimulating the user's facial nerve branches (§5). The circuits are controlled by a self-adaptive control mechanism, which accommodates individual and environment diversity. In particular, the circuit can elevate stimulation level incrementally until an appropriate level is found for a specific user. We also implement a pain control protection scheme, so that the possible pain incurred by over stimulation can be avoided (§6.1); moreover, the circuits can also automatically switch to different modes according to illumination conditions (§6.1). Further, we develop an approach to derive a person's blink frequency, so that the sampling frequency for anomaly detection can be adjusted for power saving (§6.2). Experiments show that the iBlink system could continuously work in the highest power consumption level for at least 10 hours with a lithium battery pack.

Third, we implement the entire *iBlink* system, which integrates the mechanism mentioned above and a communication function module for tele-medicine applications (§7). The related computing and control mechanisms are hosted in a Raspberry PI Zero [35] platform, which connects other hardware components such as camera and stimulation circuits. We conduct clinical trials in a hospital with our device, which enables us to obtain the design basis of *iBlink* and verify the effectiveness of our device (§9.4).

2. BACKGROUND AND MOTIVATION

Facial paralysis. A person's facial muscles are controlled by facial nerves, and a facial paralysis sufferer has a dysfunction in the facial nerve system, thus loses the facial movements. The left part of Fig. 1 shows a man with Bell's palsy on his right side of the face tries to raise his eyebrows and show his teeth [3]. It is clear that the facial muscles on his right side of face cannot move. The right part of Fig. 1 shows the anatomy of facial nerves based on [4]. The yellow and orange curves represent facial nerves of the left and right side of the face, respectively. The lesions typically occur at or beyond the stylomastoid foramen to the facial canal, which is a canal between the stylomastoid foramen and the internal acoustic meatus as shown in the right part of Fig. 1. Facial nerve branches are usually still working.

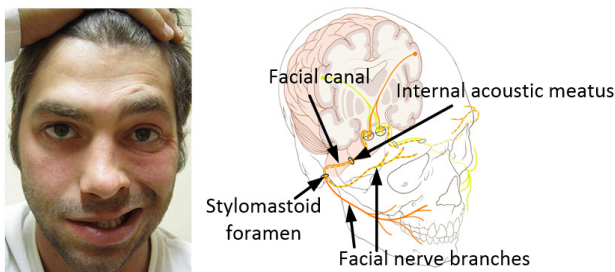


Figure 1: Anatomy of facial nerves.

The basic aim of facial rehabilitation is facial symmetry at rest and when facial expressions are performed [21]. Eye protection plays a crucial role, since patients could not blink, which makes the eye lack of moisture and protection. The

incurred complications such as corneal ulcer and lagophthalmos could further cause blindness. In clinical cases, doctors provide different treatments especially towards eye care based on an individual's expectation for recovery, degree of risk to the cornea and eye weakness [1, 9, 22].

Since a majority of Bell's palsy patients will completely recover in around 6 months, they normally take *supportive measures*, which include lubrication with artificial tears, ocular ointments and taping of the eyelid [30]. However, moisture chemicals has high risk of surface toxicity and tapes may touch the cornea or conjunctiva, which incur further trauma. *Static or dynamic surgical procedures* could be operated on prolonged and permanent paralysis sufferers. Nevertheless, such procedures involve complicated medical techniques and complications, which increase pain of patients [24, 28, 29, 31].

Electrical stimulation. Transcutaneous electrical stimulation (TENS) is taken by physiotherapists as an option for enhancing recovery in patients with facial paralysis [6, 7, 10], which is to apply electrical stimulation to facial nerves without breaking the facial skin. The electrical stimulation has been proved safe and does not interfere with recovery [6, 11, 25].

An interesting observation of electrical stimulation is: the appropriate electrical stimulation could make people blink if the facial nerve branches are not damaged. We conduct an experiment in a hospital to verify the effect, as shown in Fig. 2. The device in the left sub-figure is a Medtronic Keypoint electromyography (EMG) workstation [8], which is used to evaluate and record the electrical activity produced by skeletal muscles. The EMG workstation can generate electric current impulses, which can be directed to the person's facial skin through a pair of electrodes as shown in the middle sub-figure. By appropriately configure the strength, width and frequency of the impulse, the impulse can induce a person with functional facial nerve branches to blink as shown in the right sub-figure, where the right eye of the person is smaller than the left one as the right eye is to blink when the picture is taken.

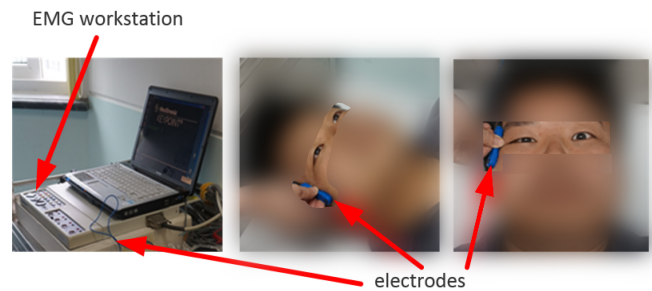


Figure 2: Electrical stimulation induced blink.

Motivation. Our work in this paper is motivated by the electrical stimulation approach for facial paralysis treatment, and the observations of facial paralysis' characteristics. Since paralysis usually occurs in one side of the face and the facial nerve branches are usually functioning, we could use electrical stimulation to make the paralyzed side to move accordingly to make the both sides of the face symmetric. In particular, the electrodes could be applied to nerve branches controlling blinks, so that the eye damage could be avoided. These functions could be implemented in a wearable smart glasses for the user's convenience, which

could improve their quality of life before the paralysis goes away completely. Moreover, the electrical stimulation approach is non-invasive, thus the device could be considered as health care products as facemasks according to the FDA regulations [5], which avoids the all-consuming license application procedures for implanting devices.

3. DESIGN AND CHALLENGES

The architecture design of *iBlink* is shown in Fig. 3, which includes hardware and software function modules.

Hardware. A camera is installed in front of the eyes to monitor blinks in real time. The eye camera captures images of both eyes and send them to the Raspberry PI Zero platform, which also monitors the ambient lighting condition. The Raspberry PI Zero and stimulation circuits are located on the patient's paralyzed side of the face. In particular, the Raspberry PI Zero and stimulation circuits are in the outer side of the glass frame, and two stimulating electrodes are in the inner side of the frame pressing on the patient's facial skin. The Raspberry PI Zero has Wi-Fi and Bluetooth interfaces which can be utilized for communication with smartphones. A power unit supports both the processing platform and the stimulation circuits. Our circuits also contain a potentiometer as the pain switch, which could fine-tuning the automatic stimulation level control scheme. This is to accommodate individual diversity in case of discomfort.

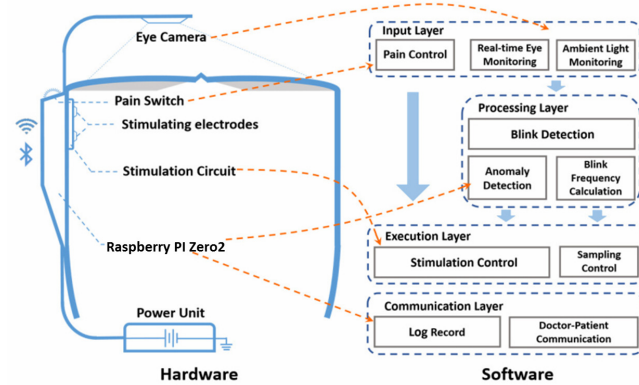


Figure 3: Design of the iBlink system

Software. The software consists of four layers: input layer, processing layer, execution layer and communication layer. The input layer receives the input images and ambient illumination data from the camera and pain control action from the pain switch. The images and illumination data are sent to the processing layer for operation model selection, blink detection, anomaly detection and blink frequency calculation. The execution layer contains stimulation control and sampling control. The stimulation control takes in the result of detections and calculations from the processing layer to adjust the electric stimulation parameters for the patient automatically. It also responds to patients' actions on the pain switch. The sampling control takes in results from the processing layer and adjusts the sampling frequency of the camera. When a doctor needs to acquire the patient's pathology data or the patient needs to report the pathology records, they can transmit data via the communication layer. The communication layer can support both Wi-Fi and Bluetooth transmissions.

Challenges. First, the system has to accommodate individual diversity. The EMG clinical trials show that different patients require different configurations of the stimulation impulse to enable blinking. The blink frequencies of different people also vary, which makes efficient blinking detection difficult. Moreover, the paralysis could make muscles around the eye droop in different degrees for different patients, which also incurs difficulties for detecting asymmetric blinks.

Second, the system has to accommodate environment changing. The patient's current conditions are monitored by the camera, thus illumination conditions could significantly influence the accuracy of the detection layer; however, the illumination conditions could change due to people's mobility and time changing. Such an un-static factor also imposes the challenge to facial expression detection.

Third, the system has to be power efficient. This is the challenge for all mobile devices. In our case, we need to lower the frequency of the power-consuming electrical impulses as much as possible. The stimulation circuits generate electrical impulses at the frequency of blink detection, while the camera has to monitor movements of the eyes at a high sampling rate to avoid information loss, which makes the sampling control a difficult trade-off and the power saving a noticeable challenge.

4. FACIAL IMAGE PROCESSING

4.1 Working Procedure

Facial image processing provides basis for blink detection, anomaly detection and blink frequency calculation, where the procedure is shown in Fig. 4. The system needs to detect whether an eye is blinking. The event that the healthy eye is blinking and the other eye is not can be detected by the anomaly detection module, which initiates the stimulation circuits. By analyzing the sequence of blink detection, the system could estimate the patient's blink frequency, so that an appropriate sampling frequency for the camera could be obtained.

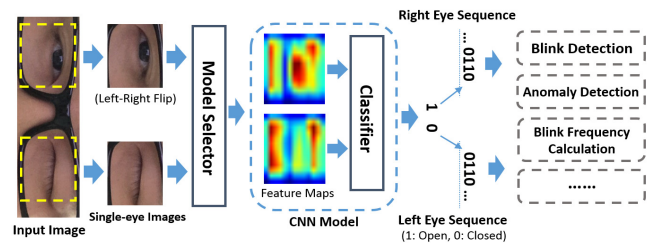


Figure 4: Workflow of facial image processing

In particular, we use two fixed windows to cut the single-eye images from the camera input for each image frame captured by the eye camera. We train the CNN model with images of the left eye and the right-to-left flip of the right eye, so that we could use just one CNN model to detect status of two eyes. Considering different illumination conditions, we train two CNN models for daytime and nighttime with IR scenarios. The model selector is to decide the images are to be processed by the model for which illumination condition. We find the threshold of model selection

through experiments, which are to be introduced in Section 9 in detail. With the extracted CNN features, we implement a classifier acting as a solver of the two-class classification problem, which labels 0 as eye closure and 1 as eye opening. A sequence of such labels could be used for detecting different events.

4.2 Deep Convolutional Neural Network

We use deep learning for image processing due to its robustness. Facial paralysis patients' eyes could sometimes be half-way open, slanted or in other more complicated shapes, thus eye images with the same 'open' label can vary greatly. Moreover, illumination, personal difference and expression can add diversity to eye images, making labeling eye images more difficult. Since high precision for our medical device is a must, we need a robust model to achieve high accuracy and high computation efficiency with different persons and under different conditions. Considering such requirements, we choose deep convolutions neural network (CNN) [17]. The details of our CNN network structure is shown in Fig. 5. We train our CNN using the deep learning framework Caffe [14].

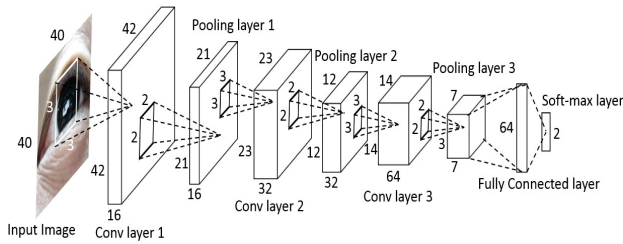


Figure 5: CNN structure

Our CNN consists of three convolutional layers and one fully connected layer. Each convolutional layer is followed by a max-pooling layer. For each convolutional layer we extract the convolved feature of previous layer's output with a linear filter. We apply multiple filters with weights W^k and bias b^k to obtain multiple feature maps. For each feature map F^k at layer k , its values are obtained by:

$$F_{ij}^k = \sigma(W^k \times x_{ij} + b^k), \quad (1)$$

where σ is a non-linear operator and x_{ij} is the input. After the convolutional layer, each feature map is sampled by the pooling layer to lower the dimension. We use the max-pooling with a non-overlapping manner. We also use ReLU [15] layers after every convolutional layer and dropout [16] layer after the third convolutional layer to improve the performance. After extracting robust features, the Softmax Loss layer computes the probability vector for classifying the images. The input for our CNN is 40×40 single-eye images.

In order to reduce the effect of local expression and personal difference in eye shapes, and to cover different illumination conditions the patients will encounter in different daily scenarios, we collected 16,951 eye images under different daylight condition and 5,750 images under IR lights from 12 different people to train the CNN models. Due to the facial symmetry, we mirrored the eye images to augment the dataset and yield 33,902 training images. We used 10% of the training data for cross validation and the other 90% for training the deep convolutional neural networks. The training accuracies for daytime and nighttime model are 99.5%

and 99.1%, respectively. We also collected another 12,000 eye images under 6 different illumination conditions for testing the two CNN models. The testing accuracies will be shown in the performance evaluation section.

4.3 Blink Detection and Anomaly Detection

After we have the eye status sequence, we define a blink sequence as a short status sequence in the form of '1,0,1', which means the eye opens, then closes and opens again. Since a normal blink takes about 200ms to 400ms and our sampling rate is 20 to 30 frames per second, there could be multiple frames captured in a normal blink process. Multiple 1s and 0s can appear in a blink sequence, e.g., '1100011'. The adjustable sampling rate of iBlink ensures that there will be at least three consecutive 0s in a normal blink sequence. Since there could be false detection on the eye status, we introduce a polling method to correctly identify a blink action. For each detection we take N_p sampling results in the eye status sequence in a sliding-window manner. If 0s are the majority in the poll, a blink will be identified. The polling method makes our system tolerant of detection exceptions in the eye status. The value of N_p is empirically set to 3 in our system.

The blink detection will be applied to both left and right eye sequences simultaneously. In most cases, people close and open their eyes at the same time, while a facial paralysis patient usually cannot close their eye on the ill-side. Consequently, if the blink detection gives a different result on two eye status sequences, we define it as an anomaly. Once an anomaly is detected, iBlink will give the patient an electrical stimulation through sending out a signal through GPIO interface of the Raspberry PI Zero.

5. STIMULATION CIRCUITS

The stimulation circuits are consisted of an amplifying circuit and a level control circuit. The amplifying circuit takes in pulse width modulation (PWM) waves from the Raspberry Pi Zero and amplifies them to generate the stimulation output on the stimulating electrodes. The level control circuit implements 16 different output stimulation levels on the stimulating electrodes by adjusting the power level of the amplified PWM waves according to the control signals from the Raspberry Pi Zero and the input from the pain switch. The working procedure of the stimulation circuits is shown in Fig. 6.

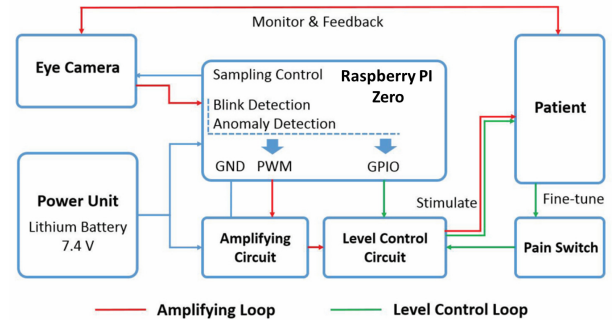


Figure 6: Workflow of the stimulation module.

The amplifying circuit takes in 3.3V PWM waves from the Raspberry PI Zero and 7.4V power input from the power

unit. In the red amplifying loop, the camera monitors the feedback of the patient after every stimulation. The Raspberry PI Zero sends out the PWM waves according to the result of blink detection and anomaly detection. And the amplifying circuit amplifies the PWM waves to output between 100V to 200V on the stimulating electrodes. The level control circuit takes in the GPIO signals and the fine-tuned pain switch input to adjust the level of the stimulation, which is shown in the level control loop.

Amplifying circuit. The amplifying circuit contains three bipolar junction transistors (BJTs), one transformer and several resistances to amplify the PWM waves from the Raspberry PI Zero. The lithium battery pack provides 7.4V power supply to the circuit, and a pair of finely placed stimulating electrodes are used to stimulate the patient's facial nerve branches. The implementation of the amplifying circuit is shown in the left part of Fig. 7.

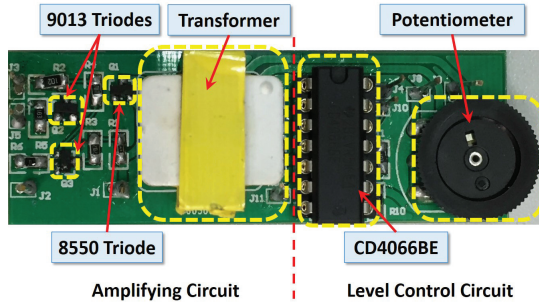


Figure 7: Circuit implementation.

We use 9013 NPN BJT triode [32] in the circuit, which is a kind of NPN low power triode mainly used for audio amplification and radio 1W push-pull output. The type of the PNP BJT is 8550 [33], which is characterized by small signal, low voltage and high current and is mainly used in switches and RF amplification. The transformer amplifies the 3.3V PWM waves to about 200V output. Although the instantaneous voltage is very high, the stimulation is safe since the high voltage lasts only in about 3 ms. For stimulating electrodes, we use electrodes made of conductive ointment, which can be finely attached to human skin and have good electrical conductivity. The distance between the two stimulating electrodes is set to be 3.3 cm, which is chosen empirically from our experiments and clinical trials to invoke the best stimulation reactions. Those conductive ointment electrodes can be easily changed for maintenance purpose on a regular basis.

Level control circuit. The level control circuit is shown in the right part of Fig. 7. It consists of a bilateral switch chip CD4066BE [34] and a potentiometer. The bilateral switch chip takes in GPIO control signals from Raspberry PI Zero and changes the output voltage level of the stimulating electrodes by switching resistances to different values. In our circuit, we implement 16 stimulation levels for the output. We also use a potentiometer as a pain switch to allow patients to adjust the output voltage manually. The potentiometer is designed to adjust the voltage only within one stimulation level in case of misoperation.

Due to unpredictable factors such as temperature, humidity and shape of human skin, conductivity of the skin varies not only among different people but also in different time

and places. It is impossible to accurately set the stimulation intensity to a fixed value; our level control circuit provides both automatic stimulation level selection and manual fine-tuning capabilities.

6. AUTOMATIC CONTROL MECHANISM

6.1 Stimulation Control

Requirements analysis. First, the conductivity of human skin varies in different situations as mentioned in the previous section, so people can have different thresholds for stimulation. We conduct clinical experiments on 5 volunteers in a hospital with the EMG workstation. The equipment we use in the hospital measures the stimulation intensity by electric current. Table. 1 shows the critical points for stimulation reactions of different patients. The values of the electric current thresholds are found by manually increasing the value by a stride of 0.1 mA, which is inconvenient and inefficient. There is a need of a mechanism that can automatically and efficiently find patients' critical points of stimulation.

Table 1: Measurement of critical points on different people

Label	Gender	Age	Critical Point (mA)
1	Female	42	5.7
2	Male	19	10.6
3	Male	35	7.0
4	Male	28	6.4
5	Female	22	4.5

Second, patients wear the iBlink on a daily basis, where the electric stimulations are applied to the patients according to the result of real-time image processing. Since the status of a human body and the surrounding environment can be changing in different times of a day, dynamically adjusting the stimulation parameters is a practical need.

Third, since human facial skin is very sensitive, in case of discomfort or pain, the iBlink needs to adjust the stimulation parameters in time according to the real-time feedback from the patients. Thus, automatic stimulation control is a must for our medical device.

Mechanism design and implementation. We define four working modes for the iBlink system:

- **Startup Mode:** When the patient wears the device for the first time and turns on the system, the iBlink automatically searches for a lowest stimulation level that can invoke an eye-closing reaction. The corresponding stimulation voltage is recorded for future use.
- **Daytime Mode:** The iBlink works in this mode when the illumination condition is good. This is the basic mode that runs in majority time of a day.
- **Nighttime Mode:** When the illumination intensity is low, iBlink starts the infrared lights and use the nighttime CNN for image processing.
- **Pain Control Mode:** This mode runs concurrently with the other four modes. Once receives the patient's signal, the iBlink automatically decreases the stimulation level to avoid pain by over stimulating.

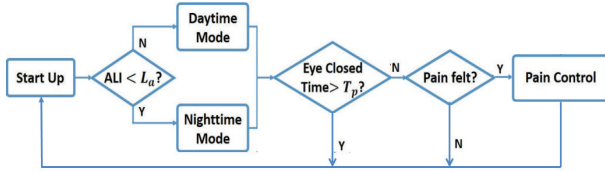


Figure 8: Working flow of automatic control mechanism.

Figure 8 shows the workflow of the automatic stimulation control, where ALI means ambient light intensity, T_p is the pain threshold. The automatic stimulation control mechanism relies mainly on the input of illumination data and blink detection results. In the startup mode, the stimulation level starts from 0 and increases incrementally. The eye camera monitors the feedback of the patient's eyes. If there is no blink resulting from the stimulation, the stimulation level continues to rise, until it reaches the level that causes an eye-closing reaction. The eye camera also monitors the illumination data, with which a model selector can switch between daytime mode and nighttime mode. In the nighttime mode, the infrared lights are turned on automatically. The infrared component emits the invisible light, which however reports no sense of discomfort either in the test on our own or in the experiments on volunteers. In case of discomfort or pain, which means there exists an over stimulating situation, the patient can give a signal by closing the healthy-side eye for a certain length of time. This triggers the pain control mode and the stimulation level starts dropping, until a new critical level is found. The pain control algorithm is shown in Algorithm 1.

Algorithm 1 Pain Control Algorithm

Require: Control Threshold C_T ; Test times k ;
Minimum Level $Level_{min}$;
Initial Level $Level_{init}$;
Ensure: Level series changing with time $Level[]$

```

1:  $k \leftarrow 1$ ,  $Level[k] \leftarrow Level_{init}$ 
2:  $t_1 \leftarrow getSystemTime()$ ,  $s_1 \leftarrow getEyeStatus()$ 
3: while True do
4:    $k \leftarrow k + 1$ 
5:    $t_2 \leftarrow getSystemTime()$ ,  $s_2 \leftarrow getEyeStatus()$ 
6:   if  $s_2 = \text{Open}$  then
7:      $s_1 \leftarrow s_2$ 
8:      $Level[k] \leftarrow Level[k - 1]$ 
9:   else
10:    if  $s_1 = \text{Open}$  then
11:       $t_1 \leftarrow t_2$ 
12:       $s_1 \leftarrow \text{Closed}$ 
13:       $Level[k] \leftarrow Level[k - 1]$ 
14:    else
15:      if  $t_2 - t_1 > C_T$  then
16:         $t_1 \leftarrow t_2$ 
17:         $Level[k] \leftarrow Level[k - 1] - 1$ 
18:        if  $Level[k] < Level_{min}$  then
19:           $Level[k] \leftarrow Level_{min}$ 
20:        end if
21:      end if
22:    end if
23:  end if
24: end while

```

6.2 Sampling Control

Normally, people can keep their eyes open for about 2 seconds to 8 seconds and then close their eyes for about 0.2 seconds to 0.4 seconds. To capture the exact movement of patients' eyes, the camera sampling frequency should be neither over low to lose useful information nor over high to consume much power. In this section, we describe our adaptive sampling algorithm which automatically adjusts the system's sampling frequency.

Upper and lower bounds of sampling interval. We set the upper bound of sampling interval B_U to be 0.05 seconds, which ensures there will be at least 3 eye-closing images captured by the camera. Since the fastest sampling frequency of our camera is 30Hz, the lower bound of the sampling interval B_L is 0.033 seconds.

Adaptive sampling algorithm. Suppose the sampling interval is τ_s , it can be expressed as

$$\tau_s = B_L + (B_U - B_L)r, \quad (2)$$

where r is a factor with $0 < r < 1$. We calculate the blink interval τ_b by averaging the time of all neighboring points of the same status in the blink graph and aggregate them into one point. The blink graph is derived by applying the polling method to the eye status sequences during blink detection. In this way, all neighboring points on blink graph are of different status. The blink interval is the time interval between two neighboring points when the eye is open. The definition of the blink interval is defined in Fig. 9.

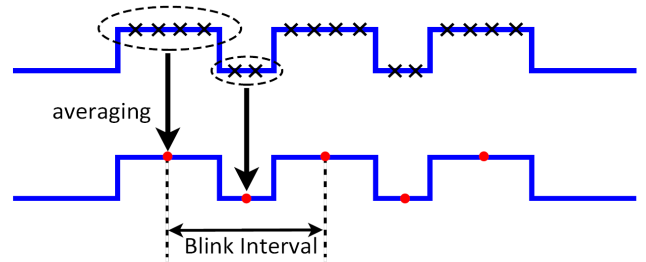


Figure 9: Definition of the blink interval

Note that there are two parameters M and α in the adaptive sampling algorithm to automatically adjust the camera sampling frequency. M is used to calculate the average period of single blink and α determines how to adjust the sampling frequency. When we are calculating the current time-interval, we look back to the past $M \cdot 2$ sampling intervals, where M is a predefined positive integer. We calculate the average of the early M blink intervals as $\bar{\tau}_b^1$ and the average of the other M intervals as $\bar{\tau}_b^2$. We set a empirical threshold τ_T and compare $\bar{\tau}_b^1$ with $\bar{\tau}_b^2$. Different events can be defined according to the comparison result:

- Advance Event: $\bar{\tau}_b^2 - \bar{\tau}_b^1 > \tau_T$, i.e., the increment of blink interval is larger than the threshold.
- Back-off Event: $\bar{\tau}_b^1 - \bar{\tau}_b^2 > \tau_T$, i.e., the decrement of blink interval is larger than the threshold.
- Stable Event: $|\bar{\tau}_b^1 - \bar{\tau}_b^2| < \tau_T$, i.e., the change of blink interval is within the threshold.

If the Advance Event is detected, the iBlink increases the sampling frequency as the patient has the tendency to increase their blink frequency. If the Back-off Event is detected, the iBlink decreases the sampling frequency.

The new r under Advance Event can be calculated as

$$r = \hat{r} - \alpha_D \hat{r}, \quad (3)$$

where $0 < \alpha_D < 1$, \hat{r} is the previous r and α_D is a constant factor controlling the rate at which r decreases.

The new r under Back-off Event can be calculated as

$$r = \hat{r} + \alpha_I(1 - \hat{r}), \quad (4)$$

where $0 < \alpha_I < 1$ and α_I is a constant factor controlling the rate at which r decreases.

The design of the formula makes r decrease slower and increase faster when it is small and increase slower and decrease faster when it is big. The parameter r will change the sampling interval accordingly. We set the initial value of r to be 0.5, which is empirically suitable for most of patients. The adaptive sampling algorithm is shown in Algorithm 2.

Algorithm 2 Adaptive Sampling Algorithm

Require: Lower bound of sampling interval B_L ;
Upper bound of sampling interval B_U ;
Parameter of sampling interval r ;
Increasing factor α_I ; Decreasing factor α_D ;
Turn count t ; Average window M .

Ensure: All sample time $S[]$;

```

1:  $t \leftarrow 1, r \leftarrow 0.5$ 
2:  $\tau_s \leftarrow B_L + (B_U - B_L)r$ 
3:  $S[0] \leftarrow 0, S[t] \leftarrow S[t-1] + \tau_s$ 
4: while True do
5:   if  $t \geq 2 \cdot M$  then
6:      $\tau_s^1 \leftarrow 0, \tau_s^2 \leftarrow 0$ 
7:     for  $i = 0 \rightarrow M$  do
8:        $\tau_s^1 \leftarrow \tau_s^1 + S[t-2M+i] - S[t-2M+i-1]$ 
9:        $\tau_s^2 \leftarrow \tau_s^2 + S[t-M+i] - S[t-M+i-1]$ 
10:    end for
11:     $\bar{\tau}_s^1 \leftarrow \tau_s^1 / M, \bar{\tau}_s^2 \leftarrow \tau_s^2 / M$ 
12:    if  $\bar{\tau}_s^2 - \bar{\tau}_s^1 > \tau_T$  then
13:       $r \leftarrow r - \alpha_D r$ 
14:    else if  $\bar{\tau}_s^1 - \bar{\tau}_s^2 > \tau_T$  then
15:       $r \leftarrow r + \alpha_I(1 - r)$ 
16:    end if
17:  end if
18:   $\tau_s \leftarrow B_L + (B_U - B_L)r$ 
19:   $t \leftarrow t + 1$ 
20:   $S[t] \leftarrow S[t-1] + \tau_s$ 
21: end while

```

7. COMMUNICATION BETWEEN THE PATIENT AND THE DOCTOR

We develop an APP to enable the iBlink system to be linked to the smart phone. The APP could collect and analyze data of the patients and send the derived information to the doctor. The doctor can request different analyzed data from the patients' devices. The communication module leverages the Wi-Fi interface of Raspberry PI Zero. The screenshots of the APP is shown in Fig. 10, from left to right is the data request page, data analysis page and its zoomed in view.

The three buttons on the data request page stand for three ways to transmit data. The "Hour" button starts a thread to request all the current day's saved data from the patient, stores them in a file and append newly collected data to the file every hour. The "Day" button will request the previous day's data and save them in a file. The "All" button will request all the data on the server and save them in files identified by date.

The data analysis page shows the blink data in a blink graph and gives data analysis result, *e.g.* blink times per day, minimum blink interval and maximum blink interval. The data are recorded to help doctors to better study the patients' pathology features.

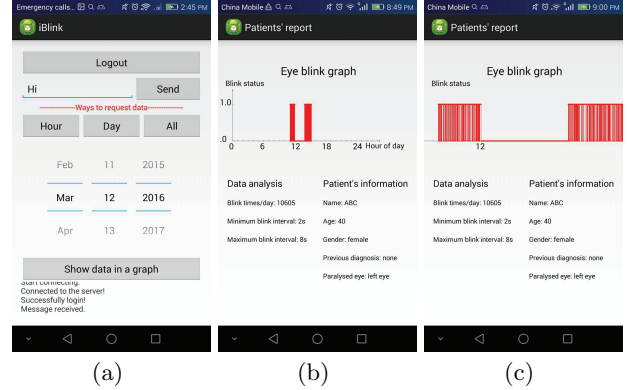


Figure 10: (a) Data request page. (b) Data analysis page. (c) Data analysis page (Zoomed in).

Since sometimes intervals of blinks can be useless, like when the eye is closed due to sleep or rest for a long time, we devise a way to detect effective time interval during a day. If any time interval between two blinks is longer than a predefined value, that interval will be discarded and not be stored in the record. The process is illustrated in Fig. 11. The predefined value is empirically chosen to be 10 seconds.

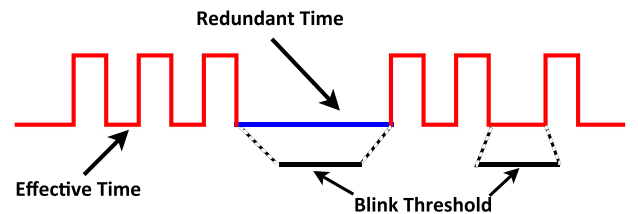


Figure 11: Effective time selection.

8. SYSTEM IMPLEMENTATION

The components of the system are tabulated in Table 2. Figure. 12(a) shows the main components of the iBlink smart glasses. The iBlink prototype is consisted of Raspberry PI Zero, stimulation circuits, stimulating electrodes, an eye camera with infrared light unit and a power unit. We use Raspberry PI Zero as the main processor. The infrared light unit is installed on the USB eye camera and powered by the GPIO output from Raspberry PI Zero. We design our own stimulation circuits with amplifying and level control circuit

embedded. The pain switch is implemented by a potentiometer to fine-tune the voltage output on the stimulating electrodes. The power unit is a 7.4V lithium battery pack and the adjustable regulator converts 7.4V to 5V to supply the Raspberry PI Zero. For wearing comfort and convenience, we design our own spectacles frame using the state-of-art 3D print machine to eliminate the complex structure of traditional frame. The components can easily be attached to the designed spectacles frame. Figure. 12(b) shows our wearable prototype.

Table 2: Components of the system

Component	Properties
Raspberry Pi Zero 2	1GHz CPU, 512MB RAM
Eye Camera	640 * 480, 30fps
CD4066BE	$-0.5V$ to $20V$, $\pm 10mA$
9013 triode	NPN, $I_{max} = 0.5A$, $625mW$
8550 triode	PNP, $I_{max} = 0.5A$, $625mW$

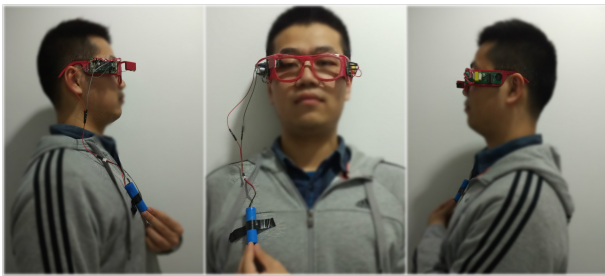
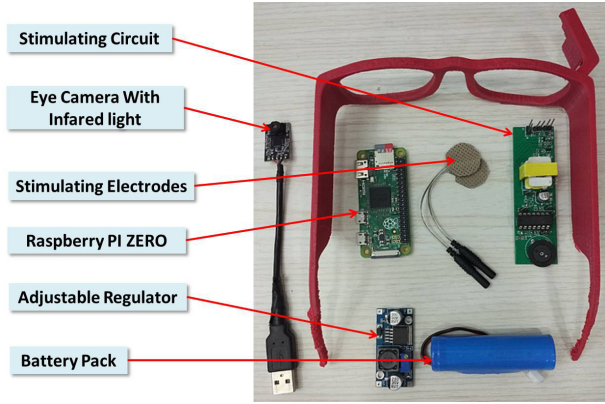


Figure 12: (a) The main components of iBlink. (b) The wearable prototype.

9. PERFORMANCE EVALUATION

9.1 Eye Status Detection

We first visualize the convolved feature maps for eye images with different status and illumination conditions, and then evaluate the performance of eye status detection by measuring the accuracy of the two CNN models.

Figure 13 shows open and closed eye images under different illumination conditions and the convolved feature maps

for each image. Row (a) shows the open eye images in different scenarios and row (b) contains the convolved feature maps after the third convolutional layer in CNN. The closed eye images and their corresponding feature maps after the third convolutional layer of CNN are shown in row (c) and row (d). The six columns demonstrate 6 different scenarios under different illumination conditions. From left to right the average illumination intensities are: less than $10lx$, $10lx$, $20lx$, $50lx$, $100lx$ and more than $1500lx$. These illumination intensities corresponds to six major scenarios a patient will encounter in daily life. Column 1 corresponds to the nighttime scenario and column 6 represents the outdoor scenario. Column 2-5 represent four different light condition in indoor scenarios: dark indoor spot, indoor on a cloudy day, room with dim light and indoor on a sunny day. For those different illumination conditions, we trained two CNN models, daytime and nighttime. The daytime model is used in outdoor scenario and indoor scenarios with sufficient light. The nighttime model is used at night and in some dark indoor scenarios with little illumination. The input images for the nighttime model are captured with the infrared lights on.

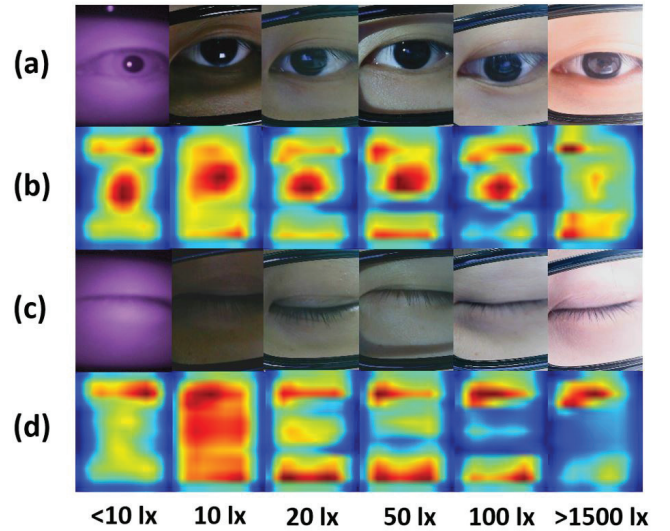


Figure 13: Eye images and convolved feature maps after the third convolutional layer.

In Fig. 13, the feature maps of open eye images in row (b) all have a circle-sized hot spot in the middle, which indicates the appearance of an eyeball, while in row (d) the closed eyes are indicated by a line figure in the feature maps.

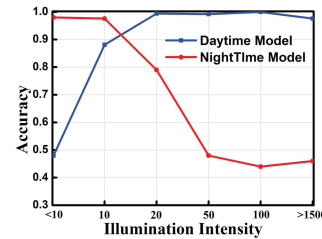


Figure 14: Eye status detection.

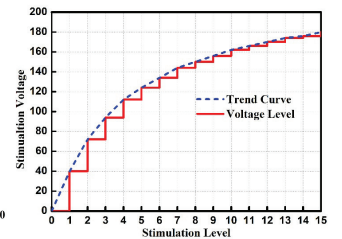


Figure 15: Voltage - Stimulation Level.

Note that in column 2 most values of the closed eye image's feature map are high, which can result in lower accuracy in the classification step. This is caused by low illumination intensity. To avoid the low accuracy, we set a threshold of $15lx$. Scenarios with lower than $15lx$ illumination intensity will be processed by the nighttime model.

Illumination is the main environment factor that influences our system's performance. We conduct experiments both in the laboratory and in the wild under different illumination conditions. The eye status detection accuracies of daytime model and nighttime model are shown in Fig. 14. We collected 500 open eye images and 500 closed eye images for each illumination condition in both normal and infrared version from 5 different people as the test data (12000 in total). With the illumination intensity over $20lx$, the daytime model's accuracy is very close to 100%. When the illumination condition reaches more than $1500lx$, the accuracy slightly drops due to the existence of some extreme cases, i.e., the illumination intensity reaches more than $10000lx$. Since those extreme cases are rare and unlikely, our daytime model satisfies patients' needs in daily scenarios. When the illumination intensity drops to under $20lx$, the nighttime model performs much better than the daytime model. In scenarios like dark indoor corners or corridors, the nighttime model can achieve an accuracy higher than 98%, which is 10% more than the daytime model. Due to the accuracy drop, we set a $15lx$ threshold for the model selector to ensure a high accuracy in different scenarios.

9.2 Automatic Stimulation Control

According to the clinical trial, a voltage between 100V to 200V can induce an eye-closing reaction. We divide the output voltage into 16 levels in our circuits, ranging from 0 to 184V. Figure 15 shows the output voltage for each stimulation level and the trend curve of the levels. In our circuit the stimulation levels do not divide the voltage range equally. The trend curve's slope tend to decrease when the stimulating level rises. We choose this level distribution since we need those levels with high voltages to increase slowly in case of discomfort or pain, while those with low voltages to increase fast to reach the critical point.

To test our stimulation control method in practice, we record the change of stimulation level by measuring the output voltage of the stimulating electrodes. Figure 16 shows the output stimulation level change we recorded. Our test covers all the scenarios we considered in the stimulation control. From time unit 0 to 12 is the startup phase. The stimulation level continues to rise according to the feedback from the eye camera. When it reaches the lowest level that can cause an eye-closing reaction, i.e., a critical point, the rising procedure stops and the voltage stabilizes on that stimulation level. Starting from time unit 13 to 18 is the first pain control phase. It is when the patient feels a mild pain and needs to fine-tune the voltage output. Note that the fine-tuning can increase or decrease the voltage in at most half range of the current stimulation level. The stimulation level eventually stabilizes on a voltage that is slightly smaller than the voltage of level 12.

At the 50th time unit the second pain control starts. In this pain control phase the patient feels a relatively strong pain and triggers the close-eye method. When iBlink detects the patient closes his eye for more than 3 seconds, the stimulation level starts dropping and stops at the first level that

cannot invoke the eye-closing reaction. Then the level rises back by one to the new critical level that can cause the close eye reaction. The patient then fine-tunes the voltage by the pain switch. After time unit 100, the patient simulates falling asleep. The close-eye method is again triggered. The stimulation control attempts to drop the stimulation level every several time units. When the attempted stimulation level causes an eye-closing reaction, the voltage stabilizes at the lower level. By this method, the stimulation level is always kept on the lowest level that can cause a close-eye action.

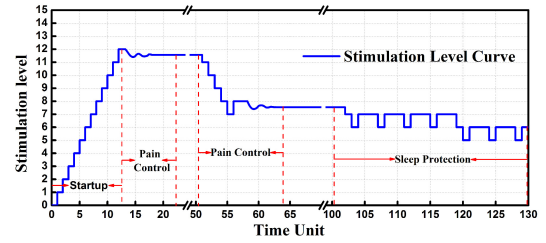


Figure 16: The change of stimulation level

9.3 Power Consumption

Power consumption is the crux of wearable devices and this also applies to iBlink. Our system uses a 7.4V lithium battery pack as the power unit, which provides power supply for both blink detection and stimulation subsystems. A natural question to ask is: how long the battery pack could support operations of the entire system. To answer this question, we conduct power consumption experiments and measure the voltage of the battery pack during the device's usage. In the experiment process, we activate the CNN based blink detection mechanisms all the time and set the highest stimulation level for the stimulation circuits. The voltage of the battery pack is measured every 10 minutes. The purpose of such a setup is to make the system operate in the highest power consumption level so that the worst case scenario can be examined. The experimental results are shown in Fig. 17, which presents how the voltage of the battery pack changes as the time goes on. It indicates that the 7.4 V lithium battery pack can support the system's operation in the worst power consumption scenario for at least 10 hours, which is sufficient for a patient's daytime use.

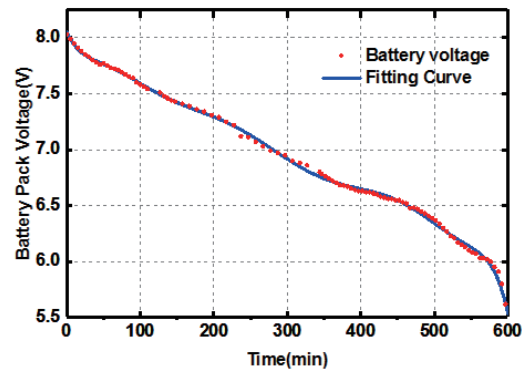


Figure 17: Power consumption.

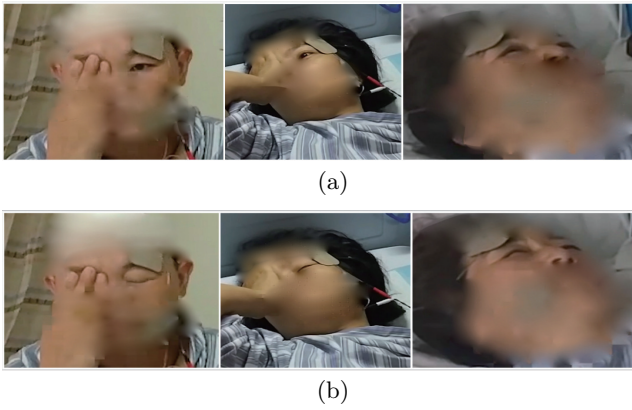


Figure 18: (a) Before stimulation. (b) After stimulation.

9.4 Experiments on Volunteers

We conduct experiments on volunteers in a hospital to verify the function of our system under the doctor’s supervision. There are six volunteers testing the stimulation circuits. We illustrate the testing snapshots of some of the patients with their permission in Fig. 18 and Fig. 19. In the process as shown in Fig. 18, the donator sticks the brown ointment electrodes to the facial nerve branches near the abnormal eye as shown in Fig. 18(a). We increase the stimulation level gradually to manually simulate the Startup Mode until the eye is stimulated to close as shown in Fig. 18(b). Table. 3 shows the critical level for stimulation of corresponding patients. All of the six patients report no feeling of pain during the whole test and only the 43-aged female volunteer mentions a slight sense of tingling. All volunteer patients appreciate our work and believe the product is useful for facial paralysis patients.

Table 3: Critical stimulation levels of different patients

Label	Gender	Age	Critical stimulation level
1	Male	21	12
2	Male	22	13
3	Female	30	7
4	Male	35	7
5	Female	43	9
6	Female	59	11

Another middle-aged female patient volunteers to try our prototype as shown in Fig. 19. The left image in Fig. 19 is the patient’s normal eye status. The camera is installed on the health left side of face and the electrodes are on the right side of her face, which is the paralyzed side. We can see that her right eye opens a little wider than the healthy side eye. The middle image is when the patient is closing her left eye while her right eye cannot be closed. This is when the iBlink sends out the stimulation signals. The right image in Fig. 19 is when the electric stimulation invokes an eye-closing reaction and the patient is able to close both of her eyes. The result of this trial proves that our device can satisfy the patient’s requirement. Note that our iBlink prototype has updated after the clinical trials in the hospital. In Fig. 19 is the previous version of the iBlink and it is used for testing

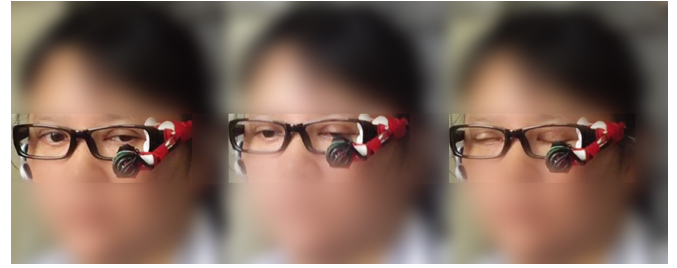


Figure 19: Experiment on Volunteers

and data collection purpose. We upgraded the iBlink to the one as shown in Fig. 12.

10. RELATED WORK

Kim *et al.* propose to use smart phones to diagnose facial paralysis [26], where the ‘asymmetric index’ is proposed to evaluate the degree of asymmetry of both sides of the face. Through measuring the asymmetric index during different expressions like resting, eye-brow raising and smiling, the smartphone could help determine if the facial paralysis happens to the person. However, the diagnosis accuracy reaches only 89%, which still needs significant improvement. In contrast to the work just propose an approach to facilitate diagnosis of facial paralysis, we implement a wearable device to provide eye protection for paralysis patients.

Wearable computing devices such as Google glasses have been attracting much attention in recent years. Efforts have been dedicated to not only design and implement new types of glasses with interesting functions, but also utilize existing equipment to carry out jobs like data collection and analysis. *iGaze*[19] and *iShadow*[18] are representatives of smart glasses proposed recently. *iGaze* establishes person-to-person as well as person-objects communication by recognizing eye gaze action. Mayberry *et al.* propose *iShadow*, where the power consumption of real-time sensing is dramatically reduced. Rallapalli *et al.* realize physical analysis in retail stores based on customer behaviors collected from smart glasses. Although smart glasses are prevailing nowadays, most existing devices just focus on entertainment. Our work in this paper focuses on eye protection for facial paralysis patients, which is an urgent requirements for a considerable group of people.

11. LIMITATIONS AND FUTURE WORK

Although the current iBlink system can realize the basic blink triggering function, considerable efforts are still needed before it can be practically deployed. The major issue of the current version of iBlink system is that the weight of the device is higher than the ordinary glasses, which makes it uncomfortable for long-time wearing. There is a need to remove some unnecessary components from the frame. Our tentative plan for the next version is to remove the Raspberry PI Zero and the eye camera from the frame and just keep the stimulation circuits and stimulating electrodes. The motivation of this revision is the observation that nowadays people spend much time watching the smartphone. We could develop a smartphone APP to learn the pattern of the user’s blink actions in the background, and the APP can send the stimulation commands to the stimulation cir-

cuits. The circuits will be enhanced with a bluetooth low energy (BLE) module to receive commands from the smart-phone and generate stimulating impulses. In this manner, the Raspberry platform and the eye camera could be removed, and it is easier to develop a graceful appearance design for the frame with remained components. In particular, the wiring overhead, and the power supply need could also be reduced, which will lay the foundation to improve the current clunky design.

12. CONCLUSION

We have designed and implemented iBlink, a pair of smart glasses to provide eye protection for facial paralysis patients. We have proposed an eye-movements detection mechanism based on deep convolutional neural network (CNN), which can detect asymmetric eye-movements of patients under various illumination conditions with an accuracy above 99%. Our library for training CNN models has been published online for further related studies, which contains more than 30,000 eye images. Moreover, we have designed and implemented an automatic stimulation circuits to generate electrical impulse for the patient's facial nerve branches stimulation, which can configure operational parameters in a self-adaptive manner for different patients. Further, we have implemented the entire *iBlink* system, which integrates the two functions above and a communication function module for tele-medicine applications. We have conducted comprehensive clinical trials in a hospital, in order to obtain the design basis and verify effectiveness of our device.

13. ACKNOWLEDGEMENTS

We sincerely appreciate our shepherd Dr. Pengyu Zhang for iteratively assisting in improving our paper. We would also like to thank the anonymous reviewers for their valuable feedback. This work is supported by National Natural Science Foundation of China (No. 61532012, 61572319, U1405251).

14. REFERENCES

- [1] National institute of neurological disorders and stroke, "Bell's Palsy Fact Sheet," Online: http://www.ninds.nih.gov/disorders/bells/detail_bells.htm
- [2] Eye image library, Online: <https://www.dropbox.com/s/vgrk4mfkpjmc0jo/EyeData.zip?dl=0>.
- [3] Picture of a Bell's palsy patient from wikipedia, Online: https://en.wikipedia.org/wiki/Bell's_palsy#/media/File:Bellspalsy.JPG.
- [4] Figure of anatomy of facial nerves, Online: https://en.wikipedia.org/wiki/Stylomastoid_foramen#/media/File:Facialcanal.png.
- [5] FDA regulations on facemasks, Online: <http://www.fda.gov/MedicalDevices/ProductsandMedicalProcedures/GeneralHospitalDevicesandSupplies/PersonalProtectiveEquipment/ucm055977.htm>.
- [6] P. Alakram and T. Puckree, "Effects of electrical stimulation in early Bell's palsy on facial disability index scores," *SA Journal of Physiotherapy*, vol. 67, no. 2, pp. 35-40, 2011.
- [7] S. M. Sandeep and V. N. Jayprakash, "Effect of electrical stimulation on facial grading system in subjects with early facial palsy," *National Journal of Integrated Research in Medicine*, vol. 4, pp. 29-32, 2013.
- [8] Electromyography, Online: <https://en.wikipedia.org/wiki/Electromyography>.
- [9] J. Cole, S. Zimmerman and S. Gerson, "Nonsurgical neuromuscular rehabilitation of facial muscle paresis," *Rubin LR (ed): The Paralyzed Face*, pp. 107-122, 1991.
- [10] D. J. Farragher, "Electrical stimulation: A method of treatment for facial paralysis," *Rose FC, Jones R, Vrbova G (eds): Neuromuscular Stimulation: Basic Concepts and Clinical Implications.*, vol. 3, pp. 303-306, 1989.
- [11] C. S. Cohan and S. B. Kater, "Suppression of neurite elongation and growth cone motility by electrical activity," *Science*, pp. 232:1638-1640, 1986.
- [12] M. C. Brown and R. L. Holland, "A central role for denervated tissues in causing nerve sprouting," *Nature*, pp. 282:724, 1979.
- [13] D. Prutchi and M. Norris, "Design and development of medical electronic instrumentation: a practical perspective of the design, construction, and test of medical devices," 2005
- [14] Y. Jia, E. Shelhamer, J. Donahue, S. Karayev, J. Long and , R. Girshick, S. Guadarrama and T. Darrell, "Caffe: Convolutional architecture for fast feature embedding," in *Proc. of the ACM International Conference on Multimedia*, pp. 675-678, 2014.
- [15] V. Nair and G. E. Hinton, "Rectified linear units improve restricted boltzmann machines," in *Proc. of ICML*, pp. 807-814, 2010.
- [16] G. E. Hinton, N. Srivastava, A. Krizhevsky, I. Sutskever and R. R. Salakhutdinov, "Improving neural networks by preventing co-adaptation of feature detectors," *arXiv preprint arXiv:1207.0580*, pp. 1988-1996, 2012.
- [17] A. Krizhevsky, I. Sutskever and G. E. Hinton, "Imagenet classification with deep convolutional neural networks," *NIPS*, pp. 1097-1105, 2012.
- [18] A. Mayberry, P. Hu, B. Marlin, C. Salthouse and D. Ganesan, "iShadow: design of a wearable, real-time mobile gaze tracker," in *Proc. of MobiSys*, pp. 82-94, 2014.
- [19] L. Zhang, X. Li, W. Huang, K. Liu, S. Zong, X. Jian, P. Feng, T. Jung, Taeho and Y. Liu, "It starts with igaze: Visual attention driven networking with smart glasses," in *Proc. of ACM/IEEE MobiCom*, pp. 91-102, 2014.
- [20] Z. Zhu and Q. Ji, "Robust real-time eye detection and tracking under variable lighting conditions and various face orientations," *Computer Vision and Image Understanding*, vol. 98, no. 1, pp. 124-154, 2005.
- [21] I. Mavrikakis, "Facial nerve palsy: anatomy, etiology, evaluation, and management," *Orbit*, vol. 27, no. 6, pp. 466-474, 2008.
- [22] U. S. Rao, J. Poll and M. T. Yen, "Prognosis for recovery vital to facial nerve palsy management," *Ophthalmology Times*, vol. 34, no. 19, pp. 24-26, 2009.
- [23] S. L. Spruance, "Bell palsy and herpes simplex

- virus," *Annals of Internal Medicine*, vol. 120, no. 12, pp. 1045, 1994.
- [24] A. K. Das, K. Sabarigirish and R. C. Kashyap, "Facial nerve paralysis: A three year retrospective study," *Indian Journal of Otolaryngology and Head and Neck Surgery*, vol. 58, no. 3, pp. 225-228, 2006.
- [25] P. Alakram and T. Puckree, "Effects of electrical stimulation on house-brackmann scores in early bells palsy," *Physiotherapy theory and practice*, vol. 26, no. 3, pp. 160-166, 2010.
- [26] H. Kim, S. Kim, Y. Kim and K. Park, "A smartphone-based automatic diagnosis system for facial nerve palsy," *Sensors*, vol. 15, no. 10, pp. 26756-26768, 2015.
- [27] H. Kim, S. Kim, Y. Kim and K. Park, "What Is Bell's Palsy?" *Harvard Women's Health Watch*, vol. 8, no. 10, pp. 8, 2001.
- [28] V. Gelder, S. Ronald and L. Gelder, "Facial expression and speech: Neuroanatomical considerations," *International journal of psychology*, vol. 25, no. 10, pp. 141-155, 1990.
- [29] H. Arion, "Dynamic closure of the lids in paralysis of the orbicularis muscle," *Plastic and Reconstructive Surgery*, vol. 50, no. 6, pp. 629, 1972.
- [30] D. Moral-Fatio and J. Laiardrie, "Palliative surgical treatment of facial paralysis. The palpebral spring," *Plastic and reconstructive surgery*, vol. 33, no. 5, pp. 446-456, 1964.
- [31] F. Masters, D. Robinson and J. Simons, "Temporalis transfer for lagophthalmos due to seventh nerve palsy," *The American Journal of Surgery*, vol. 110, no. 4, pp. 607-611, 1965.
- [32] Datasheet of 9013, Online:http://datasheet.eeworld.com.cn/pdf/WINGS/66397_9013.pdf
- [33] Datasheet of 8550, Online:http://datasheet.eeworld.com.cn/pdf/142482_STANSON_8550.html
- [34] Datasheet of CD4066BE, Online:<http://www.ti.com/lit/ds/symlink/cd4066b-mil.pdf>
- [35] Raspberry Pi user guide, Online:<https://www.raspberrypi.org/blog/raspberry-pi-user-guide-2nd-edition/>